



Identification of glutamyl-prolyl-tRNA synthetase as a new therapeutic target in hepatocellular carcinoma via a novel bioinformatic approach

Jinyong Shu^{1#}, Pan Luo^{2#}, Guifeng Zhang³, Yi Gao^{1,4}

¹General Surgery Center, Department of Hepatobiliary Surgery II, Guangdong Provincial Research Center for Artificial Organ and Tissue Engineering, Zhujiang Hospital, Southern Medical University, Guangzhou, China; ²Department of Oncology, Yueyang Central Hospital, Yueyang, China; ³Institute of Process Engineering, Chinese Academy of Sciences, Beijing, China; ⁴State Key Laboratory of Organ Failure Research, Southern Medical University, Guangzhou, China

Contributions: (I) Conception and design: J Shu; (II) Administrative support: Y Gao; (III) Provision of study materials or patients: G Zhang; (IV) Collection and assembly of data: P Luo; (V) Data analysis and interpretation: Y Gao; (VI) Manuscript writing: All authors; (VII) Final approval of manuscript: All authors.

[#]These authors contributed equally to this work.

Correspondence to: Yi Gao, MD. General Surgery Center, Department of Hepatobiliary Surgery II, Guangdong Provincial Research Center for Artificial Organ and Tissue Engineering, Zhujiang Hospital, Southern Medical University, Guangzhou, China; State Key Laboratory of Organ Failure Research, Southern Medical University, 253 Gongye Middle Avenue, Haizhu District, Guangzhou, China. Email: drgaoy@126.com; Guifeng Zhang, PhD. Institute of Process Engineering, Chinese Academy of Sciences, No.1, 2nd North Street, Zhong Guan Cun, Beijing, China. Email: gfzhang@ipe.ac.cn.

Background: Hepatocellular carcinoma (HCC) has a high incidence, and current treatments are ineffective. We aimed to explore potential diagnostic and prognostic biomarkers for HCC by conducting bioinformatics analysis on genomic and proteomic data.

Methods: Genome and proteome data were downloaded from The Cancer Genome Atlas (TCGA) and ProteomeXchange databases, respectively. Differentially expressed genes were determined using limma package. Functional enrichment analysis was conducted by Database for Annotation, Visualization, and Integrated Discovery (DAVID). Protein-protein analysis was established by STRING dataset. Using Cytoscape for network visualization and CytoHubba for hub gene identification. The gene mRNA and protein levels were validated using GEPIA and HPA, as well as RT-qPCR and Western blot.

Results: A total of 127 up-regulated and 80 down-regulated common DEGs were identified between the genomic and proteomic data. Mining 10 key genes/proteins (ACLY, ACACB, EPRS, CAD, HSPA4, ACACA, MTHFD1, DMGDH, ALDH2, and GLDC) through protein interaction networks. In addition, Glutamyl-prolyl-tRNA synthetase (EPRS) was highlighted as an HCC biomarker that is negatively correlated with survival. Differential EPRS expression analysis in HCC and paracancerous tissues showed that EPRS expression was elevated in HCC. RT-qPCR and Western blot analysis results showed that EPRS expression was upregulated in HCC cells.

Conclusions: Our results suggest that EPRS is a potential therapeutic target for inhibiting HCC tumorigenesis and progression.

Keywords: The Cancer Genome Atlas (TCGA); ProteomeXchange; glutamyl-prolyl-tRNA synthetase (EPRS); ATP citrate lyase (ACLY); heat shock protein family A member 4 (HSPA4)

Submitted Feb 17, 2023. Accepted for publication Apr 23, 2023. Published online Apr 27, 2023.

doi: 10.21037/jgo-23-247

View this article at: <https://dx.doi.org/10.21037/jgo-23-247>

Introduction

The global cancer statistics for 2020 indicated that liver cancer has become the seventh most common malignant tumor with the second highest mortality rate (1,2). Hepatocellular carcinoma (HCC) is the primary type of liver cancer (3). Although great advances have been made in treating HCC, the overall survival (OS) rate for HCC remains low. Commonly, HCC is diagnosed at a late stage, by which point limited treatment options are available. Hence, there is a need to develop new early diagnostic markers and treatment methods (4).

In recent years, many drugs targeting HCC have been developed, such as sorafenib and regorafenib. These drugs have been used to improve the efficacy of systemic HCC treatment. However, some problems exist regarding the clinical application of these drugs, including serious adverse reactions and poor efficacy in some patients. Therefore, screening for novel molecular biomarkers and developing individualized treatment options will effectively improve the clinical efficacy of these drugs, as well as the prognosis of patients with HCC.

Many genomic and proteomic databases have been made publicly available due to the broad applicability of high-throughput genomics and proteomics (5). The Cancer Genome Atlas (TCGA; <https://www.cancer.gov/about-nci/organization/ccg/research/structural-genomics/tcga>) database contains expression profile data for many tumors and various types of tumor-associated clinical information. The ProteomeXchange (<https://www.proteomexchange.org/>) database contains many proteomic results from tumor tissues and adjacent normal tissues. Bioinformatics is an interdisciplinary subject involving biology, mathematics,

and computer science that has advanced with the Human Genome Project, which is expected to greatly impact genomics, proteomics, information science, new drug development, and various other fields (6-8) and become the cornerstone of life science in the 21st century.

Glutamyl-prolyl tRNA synthetase (EPRS) belongs to the aminoacyl tRNA synthetase (AARS) superfamily, which is responsible for translating the genetic code (9,10). EPRS has been reported to interact with hsp90 to mediate the protein-protein interactions of mammalian tRNA synthetases (11). EPRS may regulate cell proliferation in estrogen receptor-positive (ER+) breast cancer cells and cancer, and silencing EPRS in breast cancer cells dysregulates many genes, including SCYL2 (12). But the role of EPRS in HCC had not been explored.

To explore potential diagnostic and prognostic biomarkers for HCC, we conducted bioinformatics analysis on genomic and proteomic data. We observed that EPRS, ATP citrate lyase (ACLY), and heat shock protein family A (Hsp70) member 4 (HSPA4) were highly expressed in HCC tissues. Moreover, all these proteins were associated with poor survival in patients with HCC. Through a literature survey, we found that EPRS has not been reported previously as a prognostic marker for HCC. We studied differential EPRS expression in fresh paired HCC tumor tissues and adjacent normal tissues from human specimens. Moreover, we constructed lentiviral vectors to knockdown or enhance EPRS expression in HepG2 cells and found that EPRS promoted cell proliferation and invasion. Thus, our current findings suggest new treatment targets for HCC. We present the following article in accordance with the MDAR and STREGA reporting checklists (available at <https://jgo.amegroups.com/article/view/10.21037/jgo-23-247/rc>).

Highlight box

Key findings

- Glutamyl-prolyl-tRNA synthetase (EPRS) expression was shown to be elevated in hepatocellular carcinoma (HCC) and maybe useful for curative effects in HCC.

What is known and what is new?

- HCC has a high incidence, and current treatments are ineffective.
- The effect of EPRS genes for HCC has been studied little.

What is the implication, and what should change now?

- EPRS is a potential therapeutic target for inhibiting HCC tumorigenesis and progression which may be used for clinical application in HCC to help clinicians to develop personalized treatment.

Methods

Dataset

We downloaded publicly available genome and proteome data from the TCGA and ProteomeXchange databases, respectively. Common differentially expressed genes and proteins (DEGPs) were identified and submitted to the Database for Annotation, Visualization, and Integrated Discovery (DAVID; <https://david.ncifcrf.gov/>) (13) for gene classification and pathway analysis. A protein-protein interaction (PPI) network of DEGPs was obtained using the Search Tool for the Retrieval of Interacting Genes/

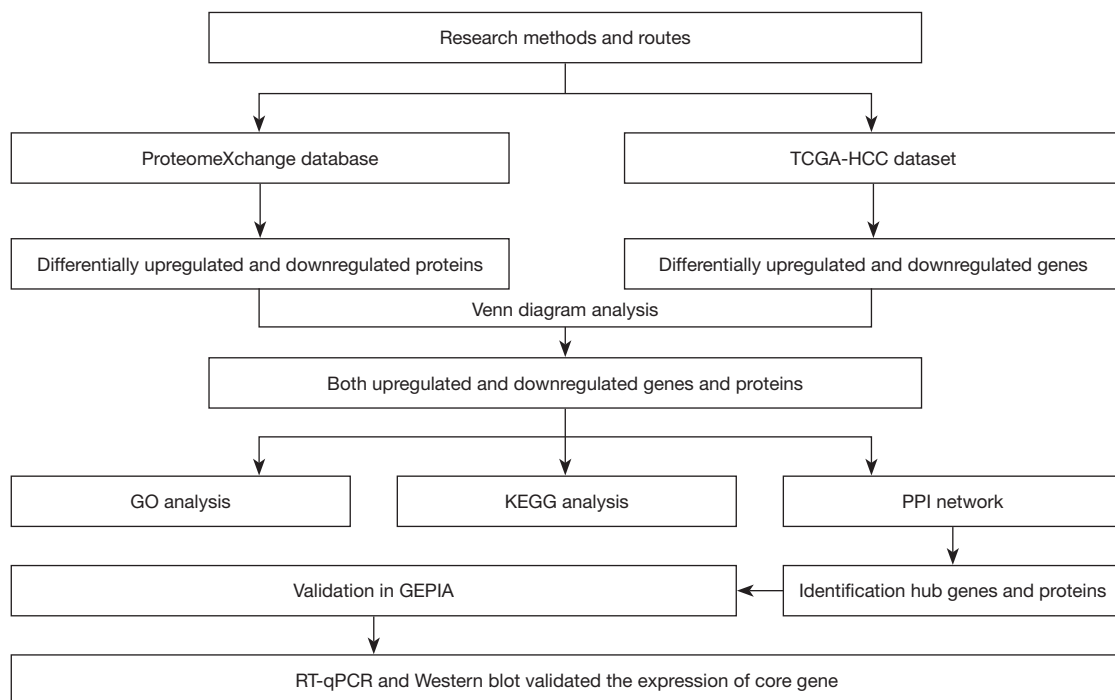


Figure 1 Flow chart. TCGA-HCC, The Cancer Genome Atlas-hepatocellular carcinoma; PPI, protein-protein interaction; GO, gene ontology; KEGG, Kyoto Encyclopedia of Genes and Genomes; GEPIA, Gene Expression Profiling Interactive Analysis; RT-qPCR, real-time reverse transcriptase-polymerase chain reaction.

Proteins (STRING; <https://string-db.org/>) database (14). The top 10 proteins with the strongest interactions were confirmed using the Cytoscape (<https://cytoscape.org/>) plug-in. The top 10 candidate factors were further screened using the Gene Expression Profiling Interactive Analysis (GEPIA; <http://gepia.cancer-pku.cn/>) database for factors that are highly expressed in tumor tissues and associated with a poor prognosis. Fresh HCC and paracancerous tissues were collected to determine the expression of the target molecules at messenger RNA (mRNA) and protein levels. Lentiviral vectors were used to knock down or enhance the expression of candidate factors in HepG2 cells and study the corresponding effects on cell proliferation, apoptosis, and invasiveness. The study design is shown in *Figure 1*. This study was approved by the Ethics Committee of Zhujiang Hospital of Southern Medical University (No. 2017-gdek-004). This study was conducted in accordance with the Declaration of Helsinki (as revised in 2013).

Patients and tissue preparation

In this study, we included 10 patients with HCC who received surgical treatment without neoadjuvant therapy

at Hunan Provincial People's Hospital from August 2019 to October 2019. Written informed consent was provided by the patients before tissue sample collection. Paired cancerous and adjacent normal tissues (2 cm apart) were collected from these patients. Intraoperative specimens were immediately frozen in liquid nitrogen and stored at -80°C until use.

Data sources

Original proteomic data for HCC and normal samples were downloaded from ProteomeXchange (<http://dx.doi.org/10.6019/PXD002171>). This dataset included protein expression information from 19 patients with HCC. Label-free proteomic analysis was performed on the 19 HCC tissues and corresponding normal tissues. Many differentially expressed proteins (DEPs) were identified between the 2 groups, and information for these DEPs was collected from published articles. Pre-processed RNA-sequencing (RNA-seq) data and the corresponding clinical information from patients with HCC were downloaded from TCGA data portal using SangerBox software (<http://vip.sangerbox.com/>) (15) in October, 2022.

Data processing and differential expression analysis

We identified 424 upregulated proteins and 121 downregulated proteins based on label-free proteomics analysis, using a P value of <0.05 and a $|\log_2 \text{fold-change (FC)}|$ value of >1 as screening criteria (16). Using FunRich (<http://www.funrich.org/>) software, the names of 545 proteins were converted to their respective gene symbols. RNA-seq data for patients with HCC were downloaded and pre-processed, after which they were analyzed using the limma software package (17,18). Genes with expression levels that met both criteria ($P < 0.05$ and $|\log_2 \text{FC}| > 1$) were considered differentially expressed genes (DEGs). DEGs were characterized using an online Venn diagram tool (<http://bioinformatics.psb.ugent.be/webtools/Venn/>).

Gene Ontology (GO), Kyoto Encyclopedia of Genes and Genomes (KEGG) pathway-enrichment analyses, and PPI network construction

Common upregulated and downregulated DEGs were analyzed using DAVID (version 6.7) to investigate GO and KEGG pathway enrichment. The STRING database was used to identify interactions between known and predicted molecules (19). In addition, Cytoscape was used to build a PPI network. A maximum number of interactive roles of 0 and a confidence score of ≥ 0.4 were set as the cut-off criteria. The corresponding proteins at the center of the protein network were considered core proteins. Core proteins may play important roles in tumor development and progression. The Cytoscape plug-in CytoHubba was used to compute connections between nodes. The importance of a node increases with increasing numbers of associated proteins. The top 10 nodes with the highest degree factors were considered key proteins (20) and were selected as candidate molecules for subsequent analysis. Statistical significance was considered when $P < 0.05$.

Identifying prognostic molecules

We conducted preliminary verification at the gene and protein levels using the GEPIA and Human Protein Atlas (HPA; <https://www.proteinatlas.org/>) databases, respectively. GEPIA is an interactive web server that enables analysis of RNA-seq data and survival. The expression levels of hub-genes and their relationship with prognosis of HCC were analyzed and demonstrated. The HPA database hosts data generated using various techniques, including antibody-based imaging, mass spectroscopy-based proteomics,

transcriptomics, and systems biology (21). By obtaining immunohistochemical (IHC) data from HCC tissues and normal liver tissues, we preliminarily verified the dysregulated expression of the hub genes and proteins identified using TCGA and Proteome Xchange databases (22).

Real-time reverse transcription polymerase chain reaction analysis

The TRIzol reagent (Invitrogen, Carlsbad, CA, USA) was used to extract total RNA from tissues and cells according to the manufacturer's instructions. Total RNA was reverse transcribed to complementary DNA (cDNA) using the PrimeScript Reverse Transcription Reagent Kit (Thermo Fisher, Waltham, MA, USA), as recommended by the manufacturer. We performed real-time reverse transcription polymerase chain reaction (qRT-PCR) using a SYBR Premix Ex TaqTM Kit to detect EPRS mRNA expression, based on the $2^{-\Delta\Delta C_t}$ method. The sequences of the primers used to detect EPRS and glyceraldehyde 3-phosphate dehydrogenase (GAPDH; internal control) expression were as follows: EPRS forward: 5'-GCCTTCAGGGACAGTAAGCA-3', EPRS reverse: 5'-ATGAAGTTGCTGCACAAGGG-3'; GAPDH forward 5'-CAATGACCCCTTCATTGACC-3', and GAPDH reverse 5'-GACAAGCTTCCCGTTCTCAG-3'. The relative expression levels of EPRS mRNA were determined as the ratio of EPRS mRNA to GAPDH mRNA.

Western blot and image analyses

Proteins were extracted from paired HCC and adjacent normal tissues, as well as HepG2 cells, as previously reported (11). Protein concentrations were measured with a BCA Protein Assay Kit (Abcam, London, UK). Protein expression levels in each sample were examined by western blotting. A total of 10 μg of protein were separated by sodium dodecyl sulfate-polyacrylamide gel electrophoresis (SDS-PAGE) using 12% polyacrylamide gels. The proteins were transferred to nitrocellulose membranes and blocked in 5% non-fat milk for 1 hour at 20–24 °C. Next, the nitrocellulose membranes were incubated with an anti-EPRS antibody (1:10,000; ab31531; Abcam) and an anti-rabbit IgG antibody (1:5,000; 074-1506; KPL, USA), following the manufacturer's instructions. ImageQuant image-analysis software (Cytiva; GE Healthcare Biosciences, Piscataway, NJ, USA) was used to determine the intensities of the protein bands. β -actin expression was

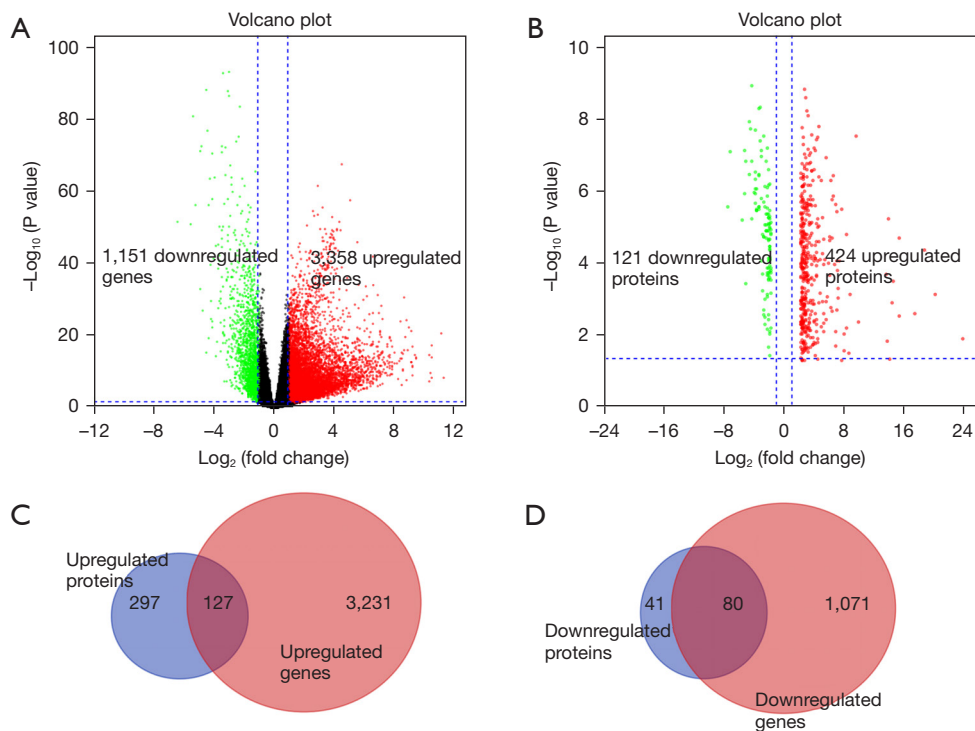


Figure 2 Data processing and differential expression analysis. Volcano plots of proteins (A) and genes (B) in HCC tissues and adjacent normal tissues. The black dots in the figures represent genes or protein that do not show significant differences. Common upregulated (C) and downregulated (D) proteins or genes. The red circles represent genes, and the blue circles represent proteins. HCC, hepatocellular carcinoma.

detected by probing with an anti- β -actin antibody (1:5,000; 60009-1-Ig; Proteintech, Rosemont, IL, USA) and used as a loading control.

Statistical analysis

All statistical analyses were performed using the R software (v3.6.3; <https://www.r-project.org/>). Statistical significance was considered when $P < 0.05$.

Results

Common DEGs between the TCGA and ProteomeXchange datasets

Volcano plots have been used to visualize the distributions of genes or proteins between cancerous and normal tissues in different studies. The red and green dots in *Figure 2* represent genes or proteins that were significantly upregulated or downregulated, respectively. *Figure 2A* shows DEPs between HCC tumor tissues and adjacent normal tissues, where 424

were upregulated and 121 were downregulated proteins were identified using the proteomic data. *Figure 2B* shows DEGs in the TCGA dataset between HCC tumor tissues and adjacent normal tissues, including 3,357 upregulated genes and 1,151 downregulated genes. A total of 127 upregulated and 80 downregulated common DEGs were identified between the 2 datasets (*Figure 2C, 2D*).

GO, KEGG pathway analysis, and PPI network of common regulated DEGs

The detailed results of the GO and KEGG pathway analyses, GO analysis showed that the upregulated proteins were mainly enriched for the following cellular component (CC) terms: basement membrane, melanosome, nuclear chromosome, telomeric region, other organism cell, peroxisomal membrane, sarcoplasm, and mitotic spindle. The downregulated proteins were mainly enriched for the terms peroxisome, mitochondrial matrix, cortical actin cytoskeleton, tertiary granule lumen, and oxidoreductase complex (*Figure 3A*). Regarding molecular functions

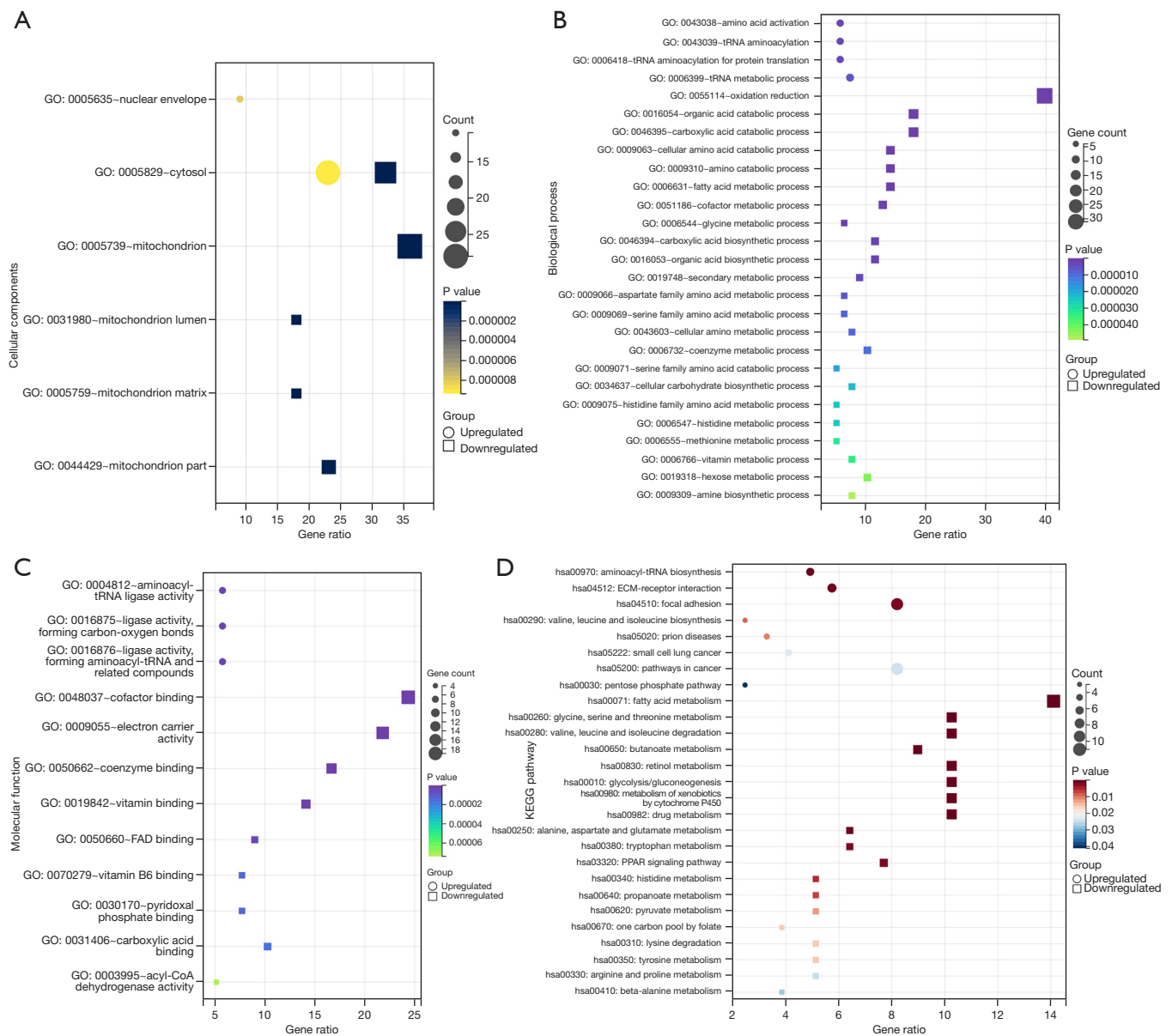


Figure 3 GO analysis, KEGG pathway-enrichment analyses, and PPI network construction. (A) Cellular components of upregulated and downregulated genes/proteins; (B) molecular functions of upregulated and downregulated genes/proteins; (C) biological pathway functions of upregulated and downregulated genes/proteins; (D) KEGG pathway analysis of the upregulated and downregulated genes/proteins. GO, Gene Ontology; KEGG, Kyoto Encyclopedia of Genes and Genomes; PPI, protein-protein network.

(MF), the upregulated proteins were mainly enriched in the following GO terms: aminoacyl-tRNA ligase activity, cadherin binding, ionotropic glutamate receptor binding, heat shock protein binding, and MHC protein complex binding. The downregulated proteins were mainly enriched for the terms c-acyltransferase activity, protein complex binding, NAD or NADH binding, vitamin binding,

coenzyme binding, ligase activity, forming carbon-sulfur bonds, and carboxylic acid binding (Figure 3B). In terms of biological pathway (BP) functions, the upregulated proteins were mainly enriched for the GO terms protein tetramerization, positive regulation of nucleocytoplasmic transport, mitotic nuclear envelope disassembly, nicotinamide nucleotide metabolic process, and steroid

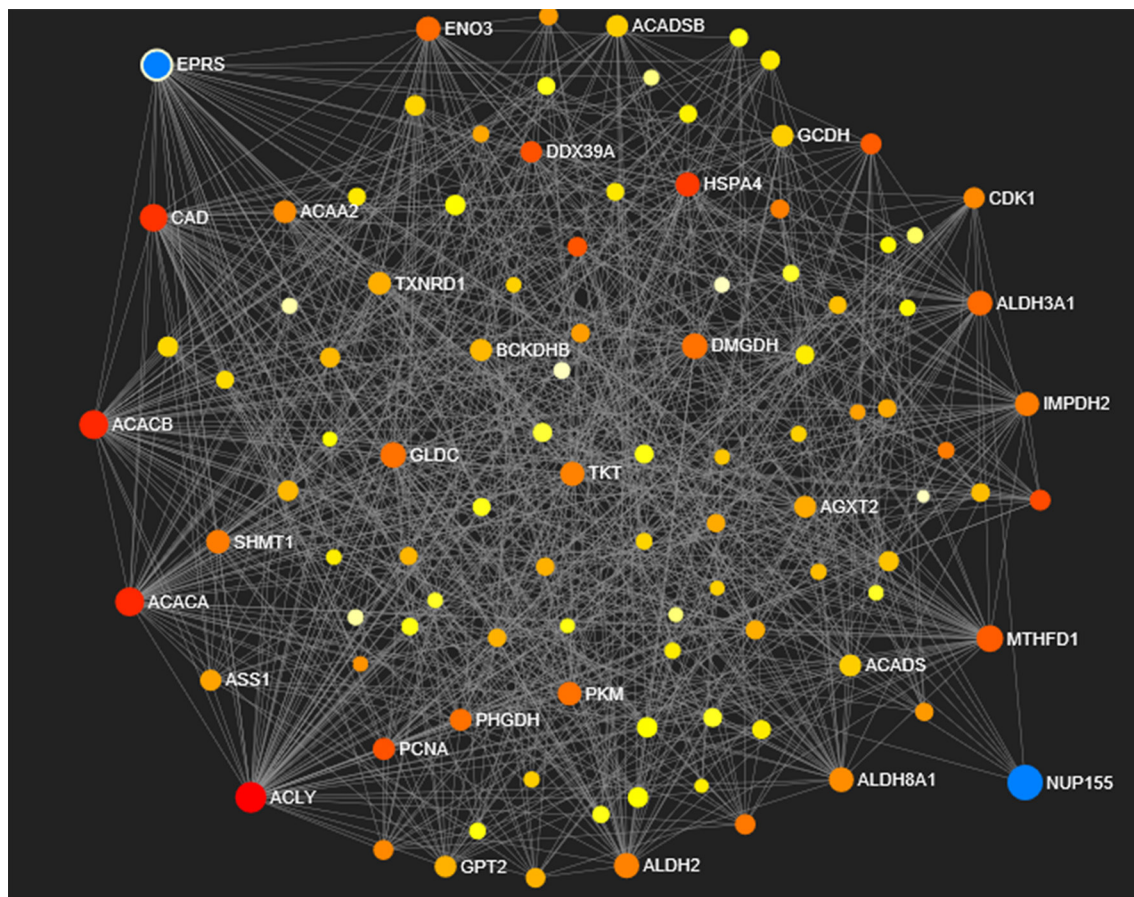


Figure 4 PPI network of the DEPGs. Each node represents a protein, an edge between two nodes represents some kind of relationship between them. The more connections of a node show, the more significant it is in the PPI network. PPI, protein-protein network; DEPGs, differentially expressed proteins and genes.

biosynthetic process. The downregulated proteins were mainly enriched for the terms cofactor metabolic process, cell amino acid metabolic process, aspartate family amino acid metabolic process, alpha-amino acid metabolic process, and organic acid catabolic process (Figure 3C). KEGG database analysis revealed that the common upregulated genes and proteins were mainly enriched for the terms extracellular matrix (ECM)-receptor, central carbon metabolism in cancer, and aminoacyl-tRNA biosynthesis. The common downregulated genes and proteins were mainly enriched for the terms fatty acid metabolism, glycine, serine, and threonine metabolism, valine, leucine, and isoleucine degradation, butanoate metabolism, retinol metabolism, glycolysis/gluconeogenesis, metabolism of xenobiotics by cytochrome P450, and drug metabolism (Figure 3D).

The PPI network of DEPGs is shown in Figure 4. In the PPI network, each node represents a molecule and connections between the nodes represent interactions between these biomolecules. These data can be used to identify protein interactions and pathway relationships in HCC. The Cytoscape plug-in, CytoHubba, was used to calculate the interrelationships between the nodes. The number of molecules attached to a given node indicates its importance in HCC development. Using the default parameters for the top 10 nodes, 10 molecules were identified as candidate genes/proteins.

Verification of transcriptional expression and prognostic significance of key molecules based on GEPIA

We used GEPIA to visualize differences in the mRNA-

expression levels of the 10 candidate molecules between HCC and paired normal tissues. The expression levels of ACLY, ACACB, EPRS, and HSPA4 in HCC tissues were higher than those in normal tissues (*Figure 5A*). The expression levels of ACACA, MTHFD1, DMGDH, ALDH2, and GLDC in HCC tissues were not significantly different from those in normal tissues ($P>0.05$).

Next, we obtained prognostic information for the 10 key proteins in HCC from the GEPIA database (*Figure 5B*). The Kaplan–Meier Plotter demonstrated that higher mRNA expression of ACLY [hazard ratio (HR) high =1.6, $P=0.011$], EPRS (HR high =1.5, $P=0.017$), ACACA (HR high =1.6, $P=0.0066$), CAD (HR high =1.9, $P=0.00034$), and HSPA4 (HR high =1.5, $P=0.019$) was associated with a worse OS for HCC patients. Higher DMGDH (HR high =0.58, $P=0.0031$) and ALDH2 (HR high =0.62, $P=0.0069$) expression were associated with a better OS for HCC patients. The expression levels of ACACB (HR high =0.96, $P=0.96$), MTHFD1 (HR high =0.86, $P=0.41$), and GLDC (HR high =1, $P=0.93$) were not significantly correlated with the OS of HCC patients.

EPRS, ACLY, and HSPA4 protein expression between HCC and normal tissues based on HPA

We observed that EPRS, ACLY, and HSPA4 mRNA expression levels were higher in HCC tissues than in normal tissues. Moreover, high expression levels of these genes significantly correlated with poor OS. To compare EPRS, ACLY, and HSPA4 protein expression between tumor and normal tissues, we searched for immunohistochemical (IHC) data in the HPA database and selected 2 representative images for each protein. One image was obtained from normal liver tissue and the other one was obtained from HCC tumor tissue (*Figure 6*). The IHC staining demonstrated that some patients with HCC had higher EPRS, ACLY, and HSPA4 expression levels than healthy individuals.

EPRS expression between fresh HCC tissues and adjacent non-tumor tissues

It was previously reported that ACLY and HSPA4 expression was higher in HCC tissues than in adjacent tissues (23,24). However, the expression levels of EPRS in HCC and adjacent tissues have not been reported. Thus, we used fresh human tissue specimens to verify the differential expression of EPRS in HCC tumor tissues and adjacent non-tumor tissues. The results of qRT-PCR analysis

revealed that EPRS mRNA expression in HCC tumor tissues was significantly higher than that in paired adjacent non-tumor tissues ($P=0.0401$; *Figure 7A*). Western blot analysis indicated that EPRS was overexpressed in HCC tissues compared to that in paired normal tissues ($P=0.0484$; *Figure 7B*). These results suggest that EPRS is a potential biomarker of HCC.

Discussion

HCC is one of the most serious types of tumors. Identifying effective therapeutic targets will improve the prognosis of HCC. In this study, genomic and proteomic data for HCC were obtained from the TCGA and ProteomeXchange databases, respectively. We identified 127 upregulated and 80 downregulated proteins with common expression patterns in the TCGA dataset.

ARS was found to play a critical role in HCC carcinogenesis. GO and KEGG pathway analyses indicated that upregulated DEGs, including EPRS, leucyl-tRNA synthetase (LARS), methionyl-tRNA synthetase (MRS), valyl-tRNA synthetase (VARs), and histidyl-tRNA synthetase (HARS2) are primarily involved in aminoacyl-tRNA biosynthesis. Aminoacyl-tRNA synthetase (ARS) serves as a key enzyme in protein synthesis and binds to tRNAs and amino acid side chains. Members of the ARS family, including isoleucyl-tRNA synthetase (IARS), lysyl-tRNA synthetase (KRS), LARS, MRS, threonyl-tRNA synthetase (TARS), tryptophanyl-tRNA synthetase (TrpRS), prolyl-tRNA synthetase (PRS), aspartyl-tRNA synthetase (NARS), and EPRS, are associated with malignant tumors (25-29).

ARS catalyzes amino acid and transfer RNA (tRNA) binding so that the mRNA sequence is accurately reflected in the protein amino acid sequence. In addition to catalysis, ARS proteins are also involved in inflammation, malignancy, immune system diseases, infections, cardiovascular disease, and nervous system diseases (30,31). Previous data showed that KRS is related to the development of gastric cancer (GC) lung cancer, and melanoma (32). The 67-kDa laminin receptor (KRS-67LR) can promote the metastasis of breast cancer, lung cancer, ovarian cancer, colon cancer, prostate cancer, and lymphoma (33). LRS overexpression can promote the growth and migration of subcutaneous A549 cells in the alveolar basement of human adenocarcinoma cells (34). IARS has higher expression levels in colon cancer tissues than in normal tissues. In RKO colon cancer cells, knocking out IARS mRNA has been shown to

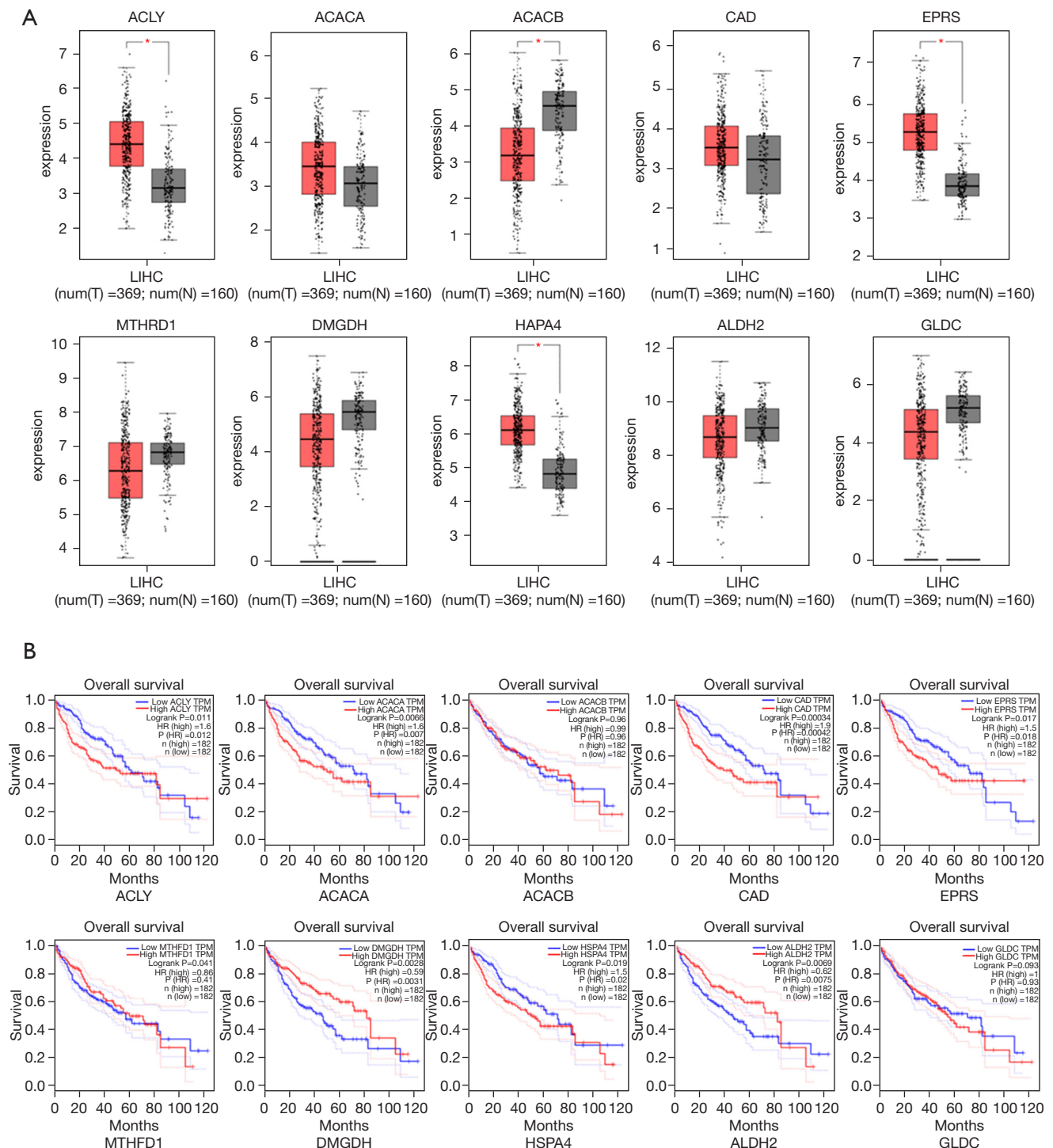


Figure 5 Expression differences of candidate genes and their relationship with prognosis. The ten genes with the highest connectivity in the PPI network were considered as candidate genes. (A) mRNA-expression levels of the indicated 10 genes in HCC and adjacent normal tissues, based on GEPIA; (B) Kaplan–Meier Plotter analysis of the same 10 genes. * $P < 0.05$ was considered to reflect a statistically significant difference. PPI, protein-protein network; mRNA, messenger RNA; GEPIA, Gene Expression Profiling and Interactive Analysis; ACLY, ATP citrate lyase; HSPA4, heat shock protein family A member 4.

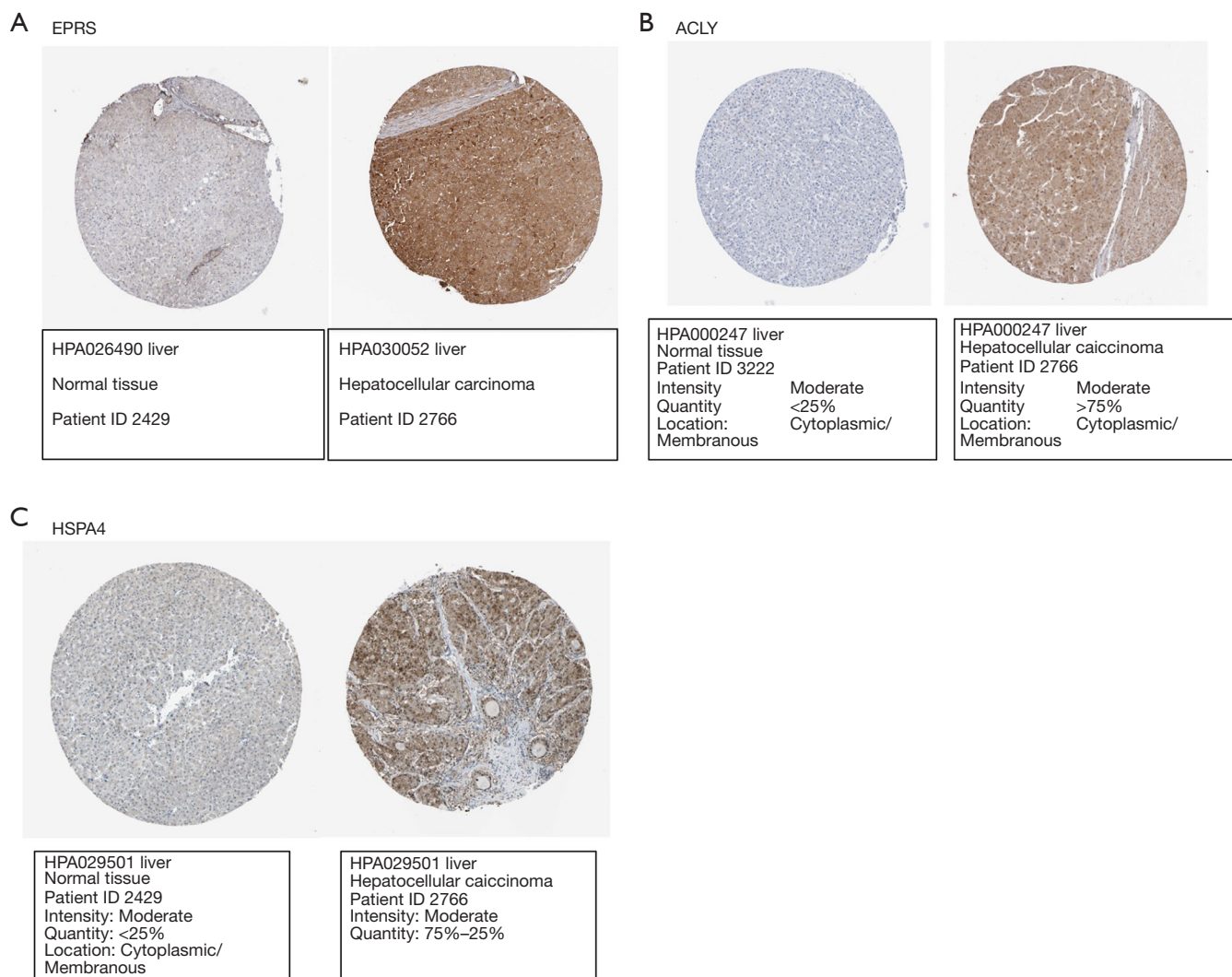


Figure 6 EPRS, ACLY, and HSPA4 proteins were higher in HCC tissues (patient ID: 2766) than in normal liver tissues using HE staining, based on information deposited in the HPA database. (A) Liver tissue with normal EPRS expression was obtained from a 55-year-old male (patient ID: 2429, https://images.proteinatlas.org/26490/54816_A_8_4.jpg and https://images.proteinatlas.org/30052/62918_B_7_7.jpg); (B) liver tissue with normal ACLY levels was obtained from a 30-year-old female (patient ID: 3222, https://images.proteinatlas.org/22959/49962_A_9_4.jpg and https://images.proteinatlas.org/28758/61505_B_7_8.jpg); (C) liver tissue with normal HSPA4 expression was collected from a 54-year-old female (patient ID: 2429, https://images.proteinatlas.org/10023/24928_A_8_4.jpg and https://images.proteinatlas.org/10023/24927_B_9_1.jpg). Magnification, $\times 200$. HCC, hepatocellular carcinoma; EPRS, glutamyl-prolyl-tRNA synthetase; ACLY, ATP citrate lyase; HSPA4, heat shock protein family A member 4; HE, hematoxylin-eosin.

inhibit cell proliferation and increased apoptosis (35). Our bioinformatics analysis revealed that EPRS, LARS, and MRS were expressed at higher levels in HCC tissues than in adjacent normal tissues, and that high EPRS, LARS, and MRS expression correlated with poor OS. These results indicate that EPRS, LARS, and MRS play important roles in HCC tumorigenesis and progression.

EPRS was identified as a potential biomarker and new therapeutic target for HCC.

The top 10 proteins with the strongest interactions were taken as candidate proteins for subsequent analysis. We verified these proteins using the GEPIA and HPA databases, and observed that only EPRS, ACLY, and HSPA4 were highly expressed in HCC and associated with

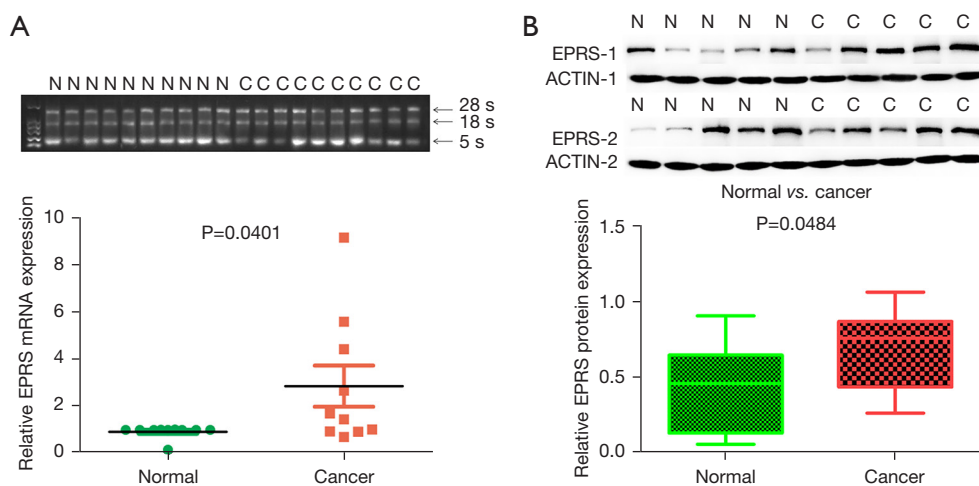


Figure 7 EPRS expression between fresh HCC tissues and adjacent non-tumor tissues. (A) EPRS mRNA was significantly upregulated ($P=0.0401$) in HCC tissues (cancer) compared with adjacent non-tumor tissues (normal). (B) EPRS protein-expression levels between HCC and adjacent normal tissues. The results indicated that EPRS was overexpressed in HCC tissues compared with that in adjacent normal tissues ($P=0.0484$). C = tumor tissue, N = adjacent normal tissue. EPRS, glutamyl-prolyl-tRNA synthetase; mRNA, messenger RNA; HCC, hepatocellular carcinoma.

poor prognosis. Considering that only EPRS has not been studied in HCC, thus we focus on EPRS.

HSPA4 is a protein-coding gene. Previous data showed that short-interfering RNA-mediated HSPA4 knockdown reduced H1299 cell migration, invasion, and transformation *in vitro* (36). HSPA4 was overexpressed in HCC and was associated with significantly worse OS or early HCC recurrence (37). ACLY is a key enzyme for *de novo* lipogenesis that is overexpressed in many tumors. Previous results showed that ACLY played an important role in HCC tumorigenesis and metastasis (38).

However, the role of EPRS in HCC remains unclear. ARSs are classical enzymes consisting of 20 evolutionarily conserved members that mediate the ligation of amino acids to their cognate tRNAs (39,40). EPRS is a cytosolic enzyme that catalyzes the synthesis of glutamyl-tRNA and prolyl-tRNA from l-glutamate and l-proline, respectively (41). The prolyl-tRNA synthetase (PRS) domain is located in the C-terminal region of EPRS and negatively affect fibrotic diseases (42), autoimmune diseases (43), and tumor progression (12,44-46). Previous data showed that EPRS can generate the fibrotic ECM via both transcriptional and translational mechanisms, suggesting that EPRS plays an important role in liver fibrosis (47), which is a main cause of HCC. In addition, EPRS can promote the production of collagen, which can promote HCC growth (48).

In this study, bioinformatic analysis showed that both

the mRNA and protein levels of EPRS were higher in HCC tissues than in adjacent normal tissues. Higher EPRS mRNA expression was found to be associated with poor OS. Fresh human tissue specimens were used to verify that EPRS was overexpressed in HCC tissues compared to adjacent normal tissues. These results indicate that EPRS may play important roles in HCC tumorigenesis and progression.

Targeted inhibition of EPRS can result in the activation of the amino acid response (AAR) signaling pathway and autophagy, thereby inhibiting cell proliferation (26) and fibrosis (47). Liu *et al.* (49) revealed that EPRS is often overexpressed in GC tissues (compared with adjacent controls), and that its overexpression is associated with a poor prognosis for patients with GC. Functionally, high EPRS expression was shown to correlate positively with GC development *in vitro* and *in vivo*. They found that angelolol (XA) and 4-hydroxyderricin (4-HD) directly bound to EPRS to block the WNT-GSK-3 β - β -catenin signaling pathway. More importantly, XA and 4-HD were shown to inhibit the growth of xenograft tumors in patients with GC and inhibited the occurrence of *Helicobacter pylori* combined with alcoholic atrophic gastritis and GC (49). Halofuginone (HF) can directly bind EPRS, which can inhibit prolyl-tRNA synthetase activity. In combination with EPRS, HF-induced autophagy suppresses the migration and invasion of MCF-7 cells by regulating the expression of STMN1 and p53 (50).

In this study, we constructed lentiviral vectors to downregulate or upregulate the expression of EPRS in HepG2 cells. The results showed that EPRS promoted HepG2 cell proliferation and invasion. However, EPRS did not significantly affect apoptosis. These findings indicate that EPRS plays a very important role in HCC progression.

At present, many inhibitors of the EPRS protein have been developed for treating fibrosis, inflammation, and tumors. The prognosis of HCC is not only related to the liver cancer progression, but also to the degree of liver fibrosis. Therefore, to improve the efficacy of HCC, it is necessary to inhibit both tumor progression and liver fibrosis progression. Therefore, EPRS is a promising therapeutic target for HCC.

Conclusions

In conclusion, our results suggest that EPRS can be used as a diagnostic and prognostic marker for HCC. Moreover, EPRS can potentially serve as a drug target to treat liver fibrosis while treating HCC, thereby further improving the therapeutic effect in patients with HCC.

Acknowledgments

We would like to thank Editage (www.editage.cn) for English language editing.

Funding: This work was supported by National Key Research and Development Program (No. 2022YFA1104900), National Natural Science Foundation of China (No. 31972926), Natural Science Foundation of Guangdong Province (No. 2023A1515012452), Basic and Applied Basic Research Foundation of Guangdong Province (No. 2023A1515012452, No. 2020A151511111), Beijing Liver-Gallbladder Xiangzhao Public Welfare Foundation (No. RGGJJ-2021-008, No. iGandanF-1082022-RGG053), the Natural Science Foundation of Guangdong Province (Nos. 2014A030312013 and 2018A030313128), the Science and Technology Program of Guangzhou (No. 201803010086), the Guangdong Key Research and Development Plan (No. 2019B020234003), and the Natural Science Foundation of Hunan Province (No. 2020JJ5560).

Footnote

Reporting Checklist: The authors have completed the MDAR and STREGA reporting checklists. Available at <https://jgo.amegroups.com/article/view/10.21037/jgo-23-247/rc>

Data Sharing Statement: Available at <https://jgo.amegroups.com/article/view/10.21037/jgo-23-247/dss>

Peer Review File: Available at <https://jgo.amegroups.com/article/view/10.21037/jgo-23-247/prf>

Conflicts of Interest: All authors have completed the ICMJE uniform disclosure form (available at <https://jgo.amegroups.com/article/view/10.21037/jgo-23-247/coif>). The authors have no conflicts of interest to declare.

Ethical Statement: The authors are accountable for all aspects of the work in ensuring that questions related to the accuracy or integrity of any part of the work are appropriately investigated and resolved. This study was conducted in accordance with the Declaration of Helsinki (as revised in 2013) and approved by the Ethics Committee of Zhujiang Hospital of Southern Medical University (No. 2017-gdek-004). Written informed consent was obtained before obtaining the tissue samples from all cases involved in the study.

Open Access Statement: This is an Open Access article distributed in accordance with the Creative Commons Attribution-NonCommercial-NoDerivs 4.0 International License (CC BY-NC-ND 4.0), which permits the non-commercial replication and distribution of the article with the strict proviso that no changes or edits are made and the original work is properly cited (including links to both the formal publication through the relevant DOI and the license). See: <https://creativecommons.org/licenses/by-nc-nd/4.0/>.

References

1. Sung H, Ferlay J, Siegel RL, et al. Global Cancer Statistics 2020: GLOBOCAN Estimates of Incidence and Mortality Worldwide for 36 Cancers in 185 Countries. *CA Cancer J Clin* 2021;71:209-49.
2. Gandhi S, Khubchandani S, Iyer R. Quality of life and hepatocellular carcinoma. *J Gastrointest Oncol* 2014;5:296-317.
3. Kim DY. New Systemic Therapies for Advanced Hepatocellular Carcinoma. *Korean J Gastroenterol* 2019;73:10-5.
4. Huang W, Skanderup AJ, Lee CG. Advances in genomic hepatocellular carcinoma research. *Gigascience* 2018;7:giy135.
5. Zhang L, Yuan L, Li D, et al. Identification of potential

- prognostic biomarkers for hepatocellular carcinoma. *J Gastrointest Oncol* 2022;13:812-21.
6. Chiou SH, Lee KT. Proteomic analysis and translational perspective of hepatocellular carcinoma: Identification of diagnostic protein biomarkers by an onco-proteogenomics approach. *Kaohsiung J Med Sci* 2016;32:535-44.
 7. Ding C, Fu X, Zhou Y, et al. Disease burden of liver cancer in China from 1997 to 2016: an observational study based on the Global Burden of Diseases. *BMJ Open* 2019;9:e025613.
 8. Yang G, Cui T, Wang Y, et al. Selective isolation and analysis of glycoprotein fractions and their glycomes from hepatocellular carcinoma sera. *Proteomics* 2013;13:1481-98.
 9. Jeong EJ, Hwang GS, Kim KH, et al. Structural analysis of multifunctional peptide motifs in human bifunctional tRNA synthetase: identification of RNA-binding residues and functional implications for tandem repeats. *Biochemistry* 2000;39:15775-82.
 10. Mendes MI, Gutierrez Salazar M, Guerrero K, et al. Bi-allelic Mutations in EPRS, Encoding the Glutamyl-Prolyl-Aminoacyl-tRNA Synthetase, Cause a Hypomyelinating Leukodystrophy. *Am J Hum Genet* 2018;102:676-84.
 11. Kang J, Kim T, Ko YG, et al. Heat shock protein 90 mediates protein-protein interactions between human aminoacyl-tRNA synthetases. *J Biol Chem* 2000;275:31682-8.
 12. Katsyv I, Wang M, Song WM, et al. EPRS is a critical regulator of cell proliferation and estrogen signaling in ER+ breast cancer. *Oncotarget* 2016;7:69592-605.
 13. Huang DW, Sherman BT, Tan Q, et al. DAVID Bioinformatics Resources: expanded annotation database and novel algorithms to better extract biology from large gene lists. *Nucleic Acids Res* 2007;35:W169-75.
 14. Szklarczyk D, Gable AL, Nastou KC, et al. The STRING database in 2021: customizable protein-protein networks, and functional characterization of user-uploaded gene/measurement sets. *Nucleic Acids Res* 2021;49:D605-12.
 15. Shen W, Song Z, Zhong X, et al. Sangerbox: A comprehensive, interaction-friendly clinical bioinformatics analysis platform. *iMeta* 2022;1:e36.
 16. Naboulsi W, Megger DA, Bracht T, et al. Quantitative Tissue Proteomics Analysis Reveals Versican as Potential Biomarker for Early-Stage Hepatocellular Carcinoma. *J Proteome Res* 2016;15:38-47.
 17. Gaudet P, Škunca N, Hu JC, et al. Primer on the Gene Ontology. *Methods Mol Biol* 2017;1446:25-37.
 18. Ritchie ME, Phipson B, Wu D, et al. limma powers differential expression analyses for RNA-sequencing and microarray studies. *Nucleic Acids Res* 2015;43:e47.
 19. Szklarczyk D, Franceschini A, Wyder S, et al. STRING v10: protein-protein interaction networks, integrated over the tree of life. *Nucleic Acids Res* 2015;43:D447-52.
 20. Hu WQ, Wang W, Fang DL, et al. Identification of Biological Targets of Therapeutic Intervention for Hepatocellular Carcinoma by Integrated Bioinformatical Analysis. *Med Sci Monit* 2018;24:3450-61.
 21. Uhlen M, Zhang C, Lee S, et al. A pathology atlas of the human cancer transcriptome. *Science* 2017;357:eaan2507.
 22. Li N, Li L, Chen Y. The Identification of Core Gene Expression Signature in Hepatocellular Carcinoma. *Oxid Med Cell Longev* 2018;2018:3478305.
 23. Yang Z, Zhuang L, Szatmary P, et al. Upregulation of heat shock proteins (HSPA12A, HSP90B1, HSPA4, HSPA5 and HSPA6) in tumour tissues is associated with poor outcomes from HBV-related early-stage hepatocellular carcinoma. *Int J Med Sci* 2015;12:256-63.
 24. Han Q, Chen CA, Yang W, et al. ATP-citrate lyase regulates stemness and metastasis in hepatocellular carcinoma via the Wnt/ β -catenin signaling pathway. *Hepatobiliary Pancreat Dis Int* 2021;20:251-61.
 25. Khan S. Recent advances in the biology and drug targeting of malaria parasite aminoacyl-tRNA synthetases. *Malar J* 2016;15:203.
 26. Kwon NH, Fox PL, Kim S. Aminoacyl-tRNA synthetases as therapeutic targets. *Nat Rev Drug Discov* 2019;18:629-50.
 27. Line A, Slucka Z, Stengrevics A, et al. Characterisation of tumour-associated antigens in colon cancer. *Cancer Immunol Immunother* 2002;51:574-82.
 28. Son SH, Park MC, Kim S. Extracellular activities of aminoacyl-tRNA synthetases: new mediators for cell-cell communication. *Top Curr Chem* 2014;344:145-66.
 29. Kim D, Kwon NH, Kim S. Association of aminoacyl-tRNA synthetases with cancer. *Top Curr Chem* 2014;344:207-45.
 30. Wang S, Yin C, Zhang Y, et al. Overexpression of ICAM-1 Predicts Poor Survival in High-Grade Serous Ovarian Carcinoma: A Study Based on TCGA and GEO Databases and Tissue Microarray. *Biomed Res Int* 2019;2019:2867372.
 31. Lee EY, Kim S, Kim MH. Aminoacyl-tRNA synthetases, therapeutic targets for infectious diseases. *Biochem Pharmacol* 2018;154:424-34.
 32. Motzik A, Amir E, Erlich T, et al. Post-translational modification of HINT1 mediates activation of MITF

- transcriptional activity in human melanoma cells. *Oncogene* 2017;36:4732-8.
33. Kim DG, Choi JW, Lee JY, et al. Interaction of two translational components, lysyl-tRNA synthetase and p40/37LRP, in plasma membrane promotes laminin-dependent cell migration. *FASEB J* 2012;26:4142-59.
 34. Shin SH, Kim HS, Jung SH, et al. Implication of leucyl-tRNA synthetase 1 (LARS1) over-expression in growth and migration of lung cancer cells detected by siRNA targeted knock-down analysis. *Exp Mol Med* 2008;40:229-36.
 35. Zhong L, Zhang Y, Yang JY, et al. Expression of IARS2 gene in colon cancer and effect of its knockdown on biological behavior of RKO cells. *Int J Clin Exp Pathol* 2015;8:12151-9.
 36. Wu CY, Lin CT, Wu MZ, et al. Induction of HSPA4 and HSPA14 by NBS1 overexpression contributes to NBS1-induced in vitro metastatic and transformation activity. *J Biomed Sci* 2011;18:1.
 37. Gu L, Zhu Y, Lin X, et al. The IKK β -USP30-ACLY Axis Controls Lipogenesis and Tumorigenesis. *Hepatology* 2021;73:160-74.
 38. Zheng Y, Zhou Q, Zhao C, et al. ATP citrate lyase inhibitor triggers endoplasmic reticulum stress to induce hepatocellular carcinoma cell apoptosis via p-eIF2 α /ATF4/CHOP axis. *J Cell Mol Med* 2021;25:1468-79.
 39. Adachi R, Okada K, Skene R, et al. Discovery of a novel prolyl-tRNA synthetase inhibitor and elucidation of its binding mode to the ATP site in complex with l-proline. *Biochem Biophys Res Commun* 2017;488:393-9.
 40. Kim S, You S, Hwang D. Aminoacyl-tRNA synthetases and tumorigenesis: more than housekeeping. *Nat Rev Cancer* 2011;11:708-18.
 41. Song DG, Kim D, Jung JW, et al. Glutamyl-Prolyl-tRNA Synthetase Regulates Epithelial Expression of Mesenchymal Markers and Extracellular Matrix Proteins: Implications for Idiopathic Pulmonary Fibrosis. *Front Pharmacol* 2018;9:1337.
 42. Wu J, Subbaiah KCV, Xie LH, et al. Glutamyl-Prolyl-tRNA Synthetase Regulates Proline-Rich Pro-Fibrotic Protein Synthesis During Cardiac Fibrosis. *Circ Res* 2020;127:827-46.
 43. Sundrud MS, Korolov SB, Feuerer M, et al. Halofuginone inhibits TH17 cell differentiation by activating the amino acid starvation response. *Science* 2009;324:1334-8.
 44. Elkin M, Ariel I, Miao HQ, et al. Inhibition of bladder carcinoma angiogenesis, stromal support, and tumor growth by halofuginone. *Cancer Res* 1999;59:4111-8.
 45. Kida Y, Taira J, Yamamoto T, et al. EprS, an autotransporter protein of *Pseudomonas aeruginosa*, possessing serine protease activity induces inflammatory responses through protease-activated receptors. *Cell Microbiol* 2013;15:1168-81.
 46. Gavish Z, Pinthus JH, Barak V, et al. Growth inhibition of prostate cancer xenografts by halofuginone. *Prostate* 2002;51:73-83.
 47. Song DG, Kim D, Jung JW, et al. Glutamyl-prolyl-tRNA synthetase induces fibrotic extracellular matrix via both transcriptional and translational mechanisms. *FASEB J* 2019;33:4341-54.
 48. Peng G, Li S, Peng Q, et al. Immobilization of native type I collagen on polypropylene fabrics as a substrate for HepG2 cell culture. *J Biomater Appl* 2017;32:93-103.
 49. Liu H, Fredimoses M, Niu P, et al. EPRS/GluRS promotes gastric cancer development via WNT/GSK-3 β / β -catenin signaling pathway. *Gastric Cancer* 2021;24:1021-36.
 50. Xia X, Wang L, Zhang X, et al. Halofuginone-induced autophagy suppresses the migration and invasion of MCF-7 cells via regulation of STMN1 and p53. *J Cell Biochem* 2018;119:4009-20.

(English Language Editor: J. Jones)

Cite this article as: Shu J, Luo P, Zhang G, Gao Y. Identification of glutamyl-prolyl-tRNA synthetase as a new therapeutic target in hepatocellular carcinoma via a novel bioinformatic approach. *J Gastrointest Oncol* 2023;14(2):636-649. doi: 10.21037/jgo-23-247